Articles in PresS. J Appl Physiol (August 22, 2003). 10.1152/japplphysiol.00303.2003

Independent Cerebral Vasoconstrictive Effects of Hyperoxia and Accompanying Arterial Hypocapnia at One ATA

Authors: Thomas F. Floyd[1], James M. Clark[2] , Robert Gelfand[2] , John A. Detre[3], Sarah Ratcliffe[4], Dimitri Guvakov[1], Christian J. Lambertsen[2], and Roderic G. Eckenhoff[1]

Affiliations: Department of Anesthesia[1], Institute for Environmental Medicine[2], Environmental Biomedical Stress Data Center[2], Department of Neurology[3], and Department of Biostatistics[4] of the University of Pennsylvania School of Medicine, Philadelphia, PA, 19104

Running Head: Cerebral Vasoconstrictive Effect of Hyperoxia

Contact Information for Corresponding Author:

Thomas F. Floyd, MD
Assistant Professor
Department of Anesthesia
Section of Cardiovascular & Thoracic Anesthesia
Hospital of the University of Pennsylvania
4-Dulles
3400 Spruce St.
Philadelphia, PA 19104-4283
(O) 215-662-3729
(F) 215-662-7106
(E) floydt@uphs.upenn.edu

Abstract:

Breathing 100% O_2 at one atmosphere absolute (ATA) is known to be associated with a decrease in cerebral blood flow (CBF). It is also accompanied by a fall in arterial pCO_2 leading to uncertainty as to whether the cerebral vasoconstriction is totally or only in part caused by arterial hypocapnia. We tested the hypothesis that the increase in arterial pO_2 while breathing O_2 at 1.0 ATA decreases CBF independently of a concurrent fall in arterial pCO_2. CBF was measured in 7 healthy men aged 21-62 years, using noninvasive CASL-Perfusion MRI. The tracer in this technique, magnetically labeled protons in blood, has a half-life of seconds, allowing repetitive measurements over short time frames without contamination. CBF and arterial blood gases were measured while breathing air, 100% O_2, and 4% CO_2 and 6% CO_2 in air and O_2 backgrounds. Arterial pO_2 increased from 91.7 ± 6.8 torr on air to 576.7 ± 18.9 torr on O_2. Arterial pCO_2 fell from 43.3 ± 1.8 torr on air to 40.2 ± 3.3 torr on O_2. CBF-arterial pCO_2 response curves for the air and hyperoxic runs were nearly parallel and separated by a distance representing a 28.7-32.6% decrement in CBF. Regression analysis confirmed the independent cerebral vasoconstrictive effect of increased arterial pO_2. The present results also demonstrate that the magnitude of this effect at 1.0 ATA is greater than previously measured.

Keywords: cerebral blood flow, oxygen, carbon dioxide, arterial spin-labeling, magnetic resonance

Introduction:

Cerebral blood flow (CBF) in normal subjects is under the continuous dominant control of arterial pCO_2 ($paCO_2$), but it can be modulated by the background level of arterial pO_2 (paO_2). Acute exposure to a high partial pressure of inspired oxygen results in a cascade of physiological events leading to increased brain tissue pCO_2, increased ventilation, decreased $paCO_2$, and decreased CBF(29, 30). The magnitude of the decrease in CBF in response to breathing 100% O_2 at 1.0 ATA, as measured by different methods, ranges from 13% to 27% of the air breathing value. Using the Kety-Schmidt method, a 13-15% decrement has been measured(27, 34), while using ^{133}Xenon scintigraphy, a 21% decrease has been reported(40). Two recently reported MRI studies using phase contrast angiography found this decrease in CBF to be in the range of 16-27%(49, 59). Since breathing oxygen, even at 1.0 ATA, is associated with arterial hypocapnia, it remains unclear as to whether the decreased CBF during hyperoxia is a consequence of the hypocapnia alone, or if there are separate effects of hypocapnia and hyperoxia. We tested the hypothesis that increase in paO_2 while breathing O_2 at 1.0 ATA decreases CBF independently of the accompanying fall in $paCO_2$, using a noninvasive MRI method to measure CBF. While the CO_2 and O_2 effects on CBF are physiologically inseparable, measurements of CBF over a range of arterial pCO_2 values in air and O_2 backgrounds made it possible to determine their separate influences analytically.

Methods:

The experimental protocol was approved by the institutional review board, and informed consent was obtained from each subject. Seven males between the ages of 21 and 62 years (Mean 39 ± 14 yrs) were studied after medical history and physical examination determined no occult cardiovascular, respiratory, neurologic or psychiatric disorder.

An open breathing system was employed to deliver mixed gases, using a low dead space, non-rebreathing valve (Hans Rudolph Model 1400), and 100-liter Douglas bag as the inspiratory reservoir. Premixed gases in high pressure cylinders containing air, 4% and 6% CO_2 in air, and 4% and 6% CO_2 in O_2 were obtained from BOC Gases (Murray Hill, N.J.). Oxygen (100% O_2) was administered from the hospital wall supply. These gases were selected to provide comparable ranges of arterial pCO_2 in air and O_2 backgrounds.

The experimental protocol was designed to minimize subject time in the magnet yet allow for stabilization of CBF after the inspired gas mixture was changed. The study was divided into two runs, an "Air" run and a "Hyperoxic" run. At the initiation of each run, a ten minute period of breathing was allowed for CBF stabilization while subjects breathed either 21% O_2 (Air run) or 100% O_2 (Hyperoxic run). Subsequently, when gases were inspired containing increasing concentrations of CO_2, a five minute period for stabilization on the new gas was allowed. A CASL-Perfusion-MRI imaging session of 6 minutes followed stabilization on each gas for the purpose of measuring CBF. CBF measurements occurred in the following order:

-'Air' Run: 1)Air → 2)Air - 4%CO_2 → 3)Air - 6%CO_2.

-'Hyperoxic' Run: 4)100%O_2 → 5)96%O_2 - 4%CO_2→ 6)94%O_2 - 6%CO_2.

For arterial blood sampling, a 22 or 20 gauge radial arterial catheter was placed using sterile technique and lidocaine 1%-2cc for local anesthesia. Arterial blood gas samples were withdrawn near the end of the 6 minute MRI scanning phase. The 3cc sample was placed in ice water and analyzed within 2-3 minutes of sampling using a NOVA pHOX analyzer (NOVA Biomedical, Waltham, MA). The following parameters were measured: pO_2, pCO_2, pH, Hgb, and Hct. Arterial blood oxygen content (CaO_2) was calculated.

The duration of each 'run' was approximately 40 minutes including time for structural imaging. Subjects were allowed a 15-30 minute rest period on air, between the two runs.

CBF measurements were made using the CASL-Perfusion MRI method (3, 12, 16). This technique has been demonstrated in humans to have a high degree of accuracy when compared to PET methods (65) as well as a high degree of precision (19). All CASL-Perfusion MRI studies were performed in a 1.5-T GE Signa Echospeed scanner (GE Medical Systems, Milwaukee, WI). CASL control labeling was applied at the level of the cervico-medullary junction using a post-labeling delay of 1.5 seconds (4). Images were acquired using a gradient-echoplanar sequence (FOV=24 x 15 cm, matrix 64x40, bandwidth 62.5 kHz, TR/TE=4000/22ms, slice thickness =8mm with a 2mm gap). Eight slices were acquired from inferior to superior in an interleaved order, and each slice acquisition took 45 ms. The imaging volume was chosen to include supratentorial structures. Each perfusion measurement consisted of 90 acquisitions with a scan time of approximately 6 minutes. Raw image data were saved onto DAT tape. A one minute

chemical shift image sequence was also performed to obtain data used for correcting geometric distortion in echoplanar images.

CASL-Perfusion MRI data were reconstructed from raw data off-line and corrected for geometric distortion using custom software written in the Interactive Data Language (IDL) software program (Research Systems, Boulder, CO). The reconstructed images in each scan were separated into 45 pairs of label and control images and then pair-wise subtracted (2). The resulting series of 45 perfusion difference images were corrected for motion and physiological fluctuation using an algorithm based on principal component analysis (5), followed by averaging across the image series to produce a single set of perfusion sensitive images.

Absolute CBF was quantified from the mean difference perfusion images using a modification of a previous approach (4) according to the following equation (12):

$$CBF = \frac{S_{CASL}\left[1-\exp\left(\frac{-TR}{T1_{CSF}}\right)\right]}{S_{CSF}\lambda\rho}\frac{\exp\left(\frac{w}{T1_a}\right)\exp\left(\frac{TE}{T2_a}\right)}{2\alpha T1_a}$$

where S_{CASL} is the difference between the control and labeled image intensities, S_{CSF} is the average intensity of the control image in the manually defined ventricular region, $T1_{CSF}$ (4.2s) is the longitudinal relaxation time of CSF, T1a and T2a are the longitudinal and transverse relaxation times of arterial blood, w is the post-labeling delay (1.5s), α is the labeling efficiency (71%), λ is the water fraction of arterial blood (0.76), and ρ is the density of brain tissue (1.05 g/mL). T1a and T2a are assumed to be constant for this study at T1a = 1100ms and T2a = 240ms. Use of fixed T1a rather than measuring tissue T1 assumes that the labeled spins remain primarily in the microvasculature rather than

exchanging completely with tissue water. However, since blood and brain T1 values are almost equal at 1.5 Tesla, violations of this assumption would cause only a small error. The CASL-Perfusion MRI technique therefore, measures the rate of microvascular blood flow within brain parenchyma (12). An example of quantitative perfusion images obtained from a six minute acquisition is shown in Fig. 1.

Global cerebral blood flow (CBF_{Global}) was determined by averaging perfusion values across all brain voxels. Secondly, brains were segmented into gray and white matter pixels based on the algorithm of Ashburner and Friston (7) within SPM 99 (1). CBF was determined for each tissue type yielding gray matter cerebral blood flow (CBF_{Gray}) and white matter cerebral blood flow (CBF_{White}).

Statistical analysis was performed using JMP® Professional software-v.5 (SAS, Cary, NC). The paired t-test was used to estimate differences in means for paired gas samples between runs. Multiple linear regression methods were used to model the contributions of baseline CBF during air breathing ($CBF_{AIR\text{-}4\%\text{-}6\%}$), change in arterial pCO_2 (ΔpCO_2), and change arterial in pO_2 (ΔpO_2), to the change in CBF (ΔCBF) when moving between the paired gases (Air - 4%CO_2 → 96%O_2 - 4%CO_2 and Air - 6%CO_2 → 94%O_2 - 6%CO_2). Terms, p-values, and power estimates are presented for this analysis.

Multiple linear and nonlinear regression approaches were also used to model the effects of baseline cerebral blood flow while breathing 21% O_2 (CBF_{AIR}), change in arterial pCO_2 from baseline on 21% O_2 (ΔpCO_2), and change in arterial pO_2 from baseline on 21% O_2 (ΔpO_2), upon CBF in gray matter, white matter, and whole brain. Coefficients of determination (R^2) are presented for the models along with p-values for

each partial regression coefficient from ANOVA. A probability of $p \leq .05$ was chosen to test significance for the whole model and for partial regression coefficients.

Results:

All subjects completed the study. Fig. 1 depicts a series of colorized CASL-Perfusion MRI image sets used for CBF measurements in a single subject. Qualitatively, from visual inspection of the images, it can be seen that CBF increases during the "Air" run with the addition of increasing inspired partial pressures of CO_2. Also, when comparing the "Air" and "Hyperoxic" runs, the matched pairs of images reveals the lower levels of CBF at all pairings in the "Hyperoxic" run.

Table 1 summarizes the pCO_2, pO_2, CaO_2 as well as CBF measurements for global (CBF_{Global}), gray (CBF_{Gray}), and white (CBF_{White}) matter regions. Breathing 100% O_2 vs. Air at one atmosphere was associated with a relative hypocapnia or decrement in arterial pCO_2 of approximately 3 torr (p=.01). The mean relative differences in CBF_{Global} in the group pairings (N=7) of Air vs. 100%O_2, Air - 4%CO_2 vs. 96%O_2 - 4%CO_2, and Air - 6%CO_2 vs. 94%O_2 - 6%CO_2 were (-)32.6% (p<.0001), (-)28.7% (p=.0008), and (-)29.4% (p<.0001), respectively. It is important to note that although there exists a statistical difference in arterial pCO_2 tensions between the Air and 100% O_2 exposures, by the addition of CO_2 at 4% and 6% inspired concentrations, we were able to eliminate any statistical differences in these levels in the subsequent comparisons.

The major goal of this study was to determine whether the effects of arterial pO_2 and pCO_2 upon CBF could be discriminated, and identify whether O_2 has a vasoconstrictive effect upon CBF independently of the mild arterial hypocapnia which occurs in response to hyperoxia in normal subjects at rest. Fig. 2 depicts graphically the relationship

between CBF and arterial pCO_2 for the seven subjects while breathing air or oxygen background gases alone and then with 4% and 6% CO_2. Two distinct, nearly parallel curves are defined. The initial points on each curve depict a difference in CBF while breathing Air vs. 100% O_2. As mentioned above, arterial pCO_2 is decreased during the transition from air breathing to O_2 breathing at 1.0 ATA resulting in the shift of the lower ('hyperoxic run') curve to the left. Any difference in CBF between these initial study points (Air vs. 100% O_2) thus reflects the combined effects of arterial hypocapnia and hyperoxia upon the cerebral vasculature (Table 1). With the addition of 4% and 6% CO_2, mean differences in arterial pCO_2 when breathing the air or hyperoxic mixtures were not significant (Table 1), and the differences between the curves at these points of comparison essentially reflect the effect of the difference in arterial pO_2 alone.

Preliminary univariate analysis indicated that the absolute magnitude and the percentage of the decrease in CBF in response to hyperoxic breathing is also dependent upon the baseline level of cerebral blood flow during air breathing (Fig. 3). Therefore, multiple regression analysis of the change in cerebral blood flow when moving from Air - $4\%CO_2 \rightarrow 96\%O_2$ - $4\%CO_2$ and Air - $6\%CO_2 \rightarrow 94\%O_2$ - $6\%CO_2$ ($\Delta CBF_{4\%-6\%}$), was conducted as a function of the initial CBF during the breathing of Air - $4\%CO_2$ or Air - $6\%CO_2$ ($CBF_{AIR-4\%-6\%}$), ΔpO_2, and ΔpCO_2 during the same transitions. A statistical summary for each of the covariates is listed in Table 2. It can be seen then that both $CBF_{AIR-4\%-6\%}$ ($p=<.0001$) and ΔpO_2 ($p=.0081$) contribute significantly to the magnitude of ΔCBF. It can also be seen that any change in arterial pCO_2 did not significantly contribute to ΔCBF as $p=.17$ for the covariate ΔpCO_2.

Thus, by comparing results at matched testing points, the decrease in CBF persists when the hypocapnia associated with breathing 100% O_2 has been eliminated (Table 1, Fig. 2). An independent cerebral vasoconstrictive effect of hyperoxia is also confirmed by using multiple regression analysis over the experimentally imposed ranges of arterial pCO_2 and pO_2 and by accounting for the impact of baseline CBF when breathing air upon the magnitude of any change.

To examine the effects of hyperoxic breathing upon different tissue types within the brain, multiple linear and nonlinear regression methods were used to analyze the contributions of the following covariates to CBF:

-$CBF_{AIR-21\%}$ - baseline CBF on air, prior to the addition of CO_2

-ΔpO_2 - change in pO_2 from baseline pO_2 on air

-ΔpCO_2 - change in pCO_2 from baseline pCO_2 on air

Regression models were created for global, gray matter, and white matter. The following equations resulted:

1) $CBF_{Global} = .62CBF_{Global\text{-}Air} - .034\Delta PO_2 + 1.5\Delta PCO_2 + 22$

Model ($R^2 = .84$, $p < .0001$)

Terms: CBF_{Air} ($p < .0001$), ΔPO_2 ($p < .0001$), ΔPCO_2 ($p < .0001$), intercept ($p < .0043$)

2) $CBF_{Gray} = .61CBF_{Gray\text{-}Air} - .048\Delta PO_2 + 1.2\Delta PCO_2 + .11\Delta PCO_2^2 + 29$

Model ($R^2 = .89$, $p < .0001$)

Terms: CBF_{Air} ($p < .0001$), ΔPO_2 ($p < .0001$), ΔPCO_2 ($p < .0001$), ΔPCO_2^2 ($P = .0088$), intercept ($p < .0012$)

3) $CBF_{White} = .73CBF_{White\text{-}Air} - .025\Delta PO_2 + .67\Delta PCO_2 + 11$

Model ($R^2 = .73$, $p < .0001$)

Terms: CBF_{Air} ($p < .0001$), ΔPO_2 ($p < .0001$),

ΔPCO_2 ($p = .0013$), intercept ($p < .029$)

Plots of actual versus predicted CBF values from the three models are further depicted in Fig. 4 (a-c). The effect of a change in arterial pO_2 could not be modeled in a nonlinear fashion as the partial pressures of oxygen created in our experimental design, essentially represent only two levels, high and low, in the presence of air breathing or 100% O_2 breathing. Nonlinear modeling of CO_2 tensions was attempted for global, gray, and white matter, and demonstrated significance when modeled as a binomial in gray matter alone.

Discussion:

Independent Cerebral Vasoconstrictive Effect of Hyperoxia

As stated previously, the normal CO_2-related interaction of respiratory and cerebral circulatory control causes the concurrent effects of hyperoxia and arterial hypocapnia to be physiologically inseparable. The linkage of these effects has been attributed to hyperventilation induced by CO_2 retention in respiratory control centers (22, 31, 33) that is in turn caused by a reduced CO_2 carrying capacity of oxyhemoglobin in association with high concentrations of physically dissolved O_2 (Haldane effect)(38). Nevertheless, the present results (Fig. 2) clearly demonstrate an independent cerebral vasoconstrictive effect of hyperoxia across a wide range of arterial pCO_2. In agreement, Kolbitsch et al (28) recently demonstrated a significant reduction in regional CBF during

oxygen breathing at 1.0 ATA when end-tidal (alveolar) pCO_2 was maintained at the air breathing control level. Reivich (45, 46) also found what appeared to be an independent vasoconstrictor effect of hyperoxia during oxygen breathing at 3.5 ATA with arterial pCO_2 maintained at about 15 torr by voluntary hyperventilation. Similar results were observed at 2.0 ATA with arterial pCO_2 maintained at about 19 torr.

In contrast to the above results, an independent vasoconstrictor effect of hyperoxia is not supported by the observations that CBF remained unchanged in normal men during the transition from air breathing to 80% O_2 at 1.0 ATA with alveolar pCO_2 controlled at 43 torr (29, 30) or in unanesthetized ponies breathing O_2 at 1.0 ATA with arterial pCO_2 maintained at air breathing control levels(10). The known association of cerebral hypoxia with extreme hypocapnia during air breathing (46) suggests that the apparent independent vasoconstrictor effect of hyperoxia found by Reivich at hypocapnic levels of arterial pCO_2 could also be explained by removal of the cerebral vasodilator effect of hypoxia(29, 45).

Analysis of the present data also demonstrates an independent vasoconstrictor effect of hyperoxia on gray and white matter CBF as well as on global CBF. The three linear models that were developed for the purpose of comparing the effects of hyperoxic breathing in global, gray, and white matter describe a greater vasoconstrictive response to increasing pO2 and greater vasodilatory response to increasing pCO2 in gray versus white matter. Gray matter is metabolically more active than white matter and thus these differences are not surprising. The higher CBF values recorded for gray matter and lower values for white matter (Table-1) are consistent with values recorded for PET (67) during air breathing. The gray/white matter CBF ratio of 1.7 from our current work is consistent

with findings in the literature from previous work using PET and SPECT of 1.6-1.8(24, 25, 41).

Oxygen in the Regulation of CBF

Mechanisms proposed as involved in the localized regulation of CBF in response to hyperoxia and hypoxia are complex, and may include roles for the parenchyma (43, 51), cerebrovascular endothelium (15, 18, 42), specific brain oxygen sensitive neurons(23), and even the RBC(17). When paO_2 is reduced by reducing the inspired pO_2, CBF does not increase until paO_2 is below 50 torr(29, 46). In contrast, CBF has been shown to inversely correlate with arterial oxygen content (CaO_2) when CaO_2 is low due to reduced hemoglobin concentration, and paO_2 is not manipulated(9). This correlation occurs whether oxygen is carried by the intact RBC or in a dissolved state(58). In the current report, there was also an inverse relation between CaO_2 and CBF. When inspired $\%O_2$ was increased from 21% to 100% at 1.0 ATA, there was a 13-14% increase in CaO_2 which was concurrent with a 33% decrease in CBF. Although these correlations exist, they do not necessarily mean that CaO_2 acts as a specific factor in brain oxygen flow control. Rather, it has been suggested that pO_2-dependent cells in endothelium may act as local oxygen sensors modulating vascular tone(44). The vasoconstrictive effect of hyperoxia may be related to inactivation of NO by enhanced generation of oxygen free radicals(44).

Magnitude of Hyperoxic Cerebral Vasoconstriction

In the present study, the transition from breathing air to 100% O_2 at 1.0 ATA caused a larger decrease in CBF (33%) than the 13-15% decrement which has been consistently reported previously (27, 34) using the Kety-Schmidt technique, or the 21%

decrease reported by Ohta (40) using ^{133}Xe scintigraphy. The present results are more consistent with, yet still larger than, the 16-27% decrease in CBF during O_2 breathing at 1.0 ATA recently reported by Watson (59) and Rostrup (49) using another MRI technique, dynamic susceptibility contrast. Even during O_2 breathing at 3.5 ATA, a previously reported CBF decrement of 25% (34) is smaller than the present value for O_2 breathing at 1.0 ATA. Only a few studies contain CBF measurements during O_2 breathing at more than one ambient pressure. Lambertsen et al. (34)found CBF decrements of 15% and 25% at 1.0 and 3.5 ATA, respectively, while Reivich (45, 46) reported values of 22% and 27% at 2.0 and 3.5 ATA in the presence of arterial hypocapnia. More recently, Ohta (40) measured CBF decrements of 9, 21, 23, and 19% at O_2 pressures of 0.5, 1.0, 1.5, and 2.5 ATA, respectively. The latter results suggest that the cerebral vasoconstrictive effect of hyperoxia may be near maximal at 1.0 ATA. At the present time, it is not practical to use CASL-Perfusion MRI or other MRI methods at ambient pressures that are greater than one atmosphere.

Comparison with Previous CBF Measurements

Quantitative investigation of cerebral blood flow and metabolism in man became possible when Kety and Schmidt developed an inert gas method for measuring CBF by calculating rate of N_2O uptake by the brain(26). The method required repeated sampling of brain venous blood from the superior bulb of the internal jugular vein concurrently with arterial blood while the subject breathed 15% N_2O for at least 10 minutes. Subsequent demonstrations that cerebral O_2 consumption is not changed by O_2 breathing at 1.0 (27, 32) or 3.5 ATA (32) made it possible to use arterial-venous O_2 content

differences across the brain to measure relative changes in CBF under these conditions(53). Continued investigation led to the development of additional CBF measurement methods that used other inert gas tracers or radioactive labels to determine rate of uptake of the tracer or rate of washout after a state of near saturation has been established(46). All of these methods require either the sampling of brain venous blood or the monitoring of brain venous concentrations of the selected tracer.

Blood from the internal jugular bulb is known to contain contributions from extra-cranial or extra-cerebral sources(52, 53). While breathing air at 1.0 ATA, extra-cranial contributions to internal jugular venous flow have been estimated to range from 3 to 7% (52), with the occasional possibility of gross contamination from extra-cranial venous effluent (35). Scheinberg (50) found that contamination of cerebral venous blood by facial or neck blood caused falsely low values of cerebral blood flow, A-V O_2 difference, and O_2 consumption. He estimated that some degree of extra-cerebral contamination occurred in about 20% of the subjects. In contrast, the CASL-Perfusion MRI technique allows CBF to be determined from designated intracranial sources by measuring the rate of microvascular blood flow within brain parenchyma(12).

It is possible, yet unlikely, that the potential extra-cerebral contamination of brain venous blood in some of the previous studies can account for the reported absence of an independent cerebral vasoconstrictive effect of hyperoxia or the smaller magnitude of this effect found previously. At the present time, there are no obvious explanations for the differences between the results of this study and those of previous investigations. In some aspects, the results of the present study are remarkably consistent with previous data. Average values of 53.6 ml/100g/min for global CBF at an arterial pCO_2 of 43.3 torr

during air breathing (Table 1) are essentially identical to corresponding values of 53 ml/100g/min and 43 torr in one of the subject groups studied by Kety and Schmidt(27). In addition, the average CBF value of 36.1 ml/100g/min at an arterial pCO_2 of 40.2 torr during O_2 breathing (Table 1) falls directly on the curve established for CBF vs arterial pCO_2 in an O_2 background while using cerebral clearance of ^{133}Xe to measure CBF(14).

Although the present CBF-arterial pCO_2 relationships for both air and O_2 breathing without added CO_2 are consistent with the results of previous studies using other methods, the slopes of the present CBF-arterial pCO_2 curves (Fig. 2) are more shallow than those found previously in normal subjects. Using A-V O_2 differences across the brain to calculate relative changes in CBF during air breathing at 1.0 ATA, Lambertsen et al. (33)found that CBF increased by 57.6% for an arterial pCO_2 increment of 8.9 torr. During air breathing in the present study, global CBF increased by 30.8% for an 8.8 torr increase in arterial pCO_2 (Table 1). Using clearance of ^{133}Xe to measure CBF during O_2 breathing with added CO_2, CBF more than doubled (102.5%) for an arterial pCO_2 increase of 11.4 torr(14). Corresponding values for the present study during O_2 breathing were 37.4% and 10.9 torr, respectively (Table 1).

Effect of CO_2 Breathing Upon Arterial pO_2

The breathing of CO_2 in an air background resulted in small increases in arterial pO_2 from 91.7 ± 6.8 torr on air to 127.0 ± 5.4 torr on Air - 4%CO_2 and 144.5 ± 6.6 torr on Air - 6%CO_2, as well as corresponding increments in CaO_2 from 17.9 ± 0.8 ml/dl on air to 18.5 ± 0.9 ml/dl on Air - 4%CO_2 and 18.7 ± 0.8 ml/dl on Air - 6%CO_2, differences which were not observed during the breathing of CO_2 in an oxygen background (Table 1). An

increase in arterial pO_2 during air breathing with added CO_2 has been attributed to increased alveolar ventilation with improved VA/Q matching (55). The present average arterial pO_2 values of 127.0 and 144.5 torr at inspired pCO_2 levels of about 28 and 43 torr agree well with previously measured values of 128.5 and 133.3 torr at controlled inspired pCO_2 levels of 30 and 40 torr, respectively(13).

CASL-Perfusion MRI

CASL Perfusion-MRI is ideally suited for this type of study at 1.0 ATA as it is completely noninvasive and the tracer, magnetically flipped protons in arterial blood, has a half-life on the order of several seconds. Multiple measurements can be obtained, over temporally short time frames, without contamination from retained tracer. Several excellent reviews have been published with detailed theoretical descriptions of the technique(8, 11, 61, 63).

The CASL-Perfusion MRI technique has been validated against "gold-standards" such as PET (37, 65) and dynamic susceptibility contrast MRI methods (36) in human brain studies. Calamante (11) offers a detailed listing of CBF measurements in various species and comparisons with those made in the same species with more traditional methods, including microspheres. Walsh (56) compared regional CBF measurements using the arterial spin-labeling technique with those obtained from radioactive microspheres in the rat and found a mean difference of 1.5%. The CASL Perfusion MRI technique has been applied clinically to study CBF in stroke (12), epilepsy (60), and Alzheimer's dementia (6), as well as blood flow in other organ systems such as lung (39, 48), kidney (47), and muscle perfusion (21). The technique has been additionally utilized

in human functional brain mapping research(62), research into human cerebral physiology (20), and in the laboratory animal for the study of blood flow in various organ systems (54, 64).

The most significant concern for CASL-Perfusion MRI is that prolonged arterial blood transit times, such as might exist in the presence of cerebrovascular disease, may cause an underestimation of flow (11). At the extreme, transit time could be greater than the time for the label to decay (T1). This deficiency has been exploited to assist in the diagnosis of cerebrovascular disease, through the noninvasive mapping of inhomogeneities in regional cerebral blood flow(57).

Conclusions:

The observed decrease in CBF while breathing 100% O_2 at 1.0 ATA represents the combined effects of arterial hyperoxia and hypocapnia. Furthermore, the present data support the hypothesis that breathing O_2 at 1.0 ATA causes cerebral vasoconstriction independently of any vasoconstriction associated with the accompanying arterial hypocapnia. These data also document that gray matter cerebral vasculature is relatively more sensitive to the vasoconstrictive properties of hyperoxia and vasodilatory properties of hypercarbia over the ranges tested. The magnitude of hyperoxia-induced cerebral vasoconstriction is considerably greater than previously reported and is highly dependent upon the magnitude of the baseline cerebral blood flow. If the systemic vasculature responds to hyperoxia in a similar degree, these results have relevance to the use of hyperoxic inspired gas mixtures as an effective means for reducing decompression stress in undersea and aerospace medicine.

Acknowledgements:

We wish to acknowledge the assistance of Julio Gonzalez, PhD, David Alsop, PhD, and Joseph Maldjian, MD for their technical assistance on this project. This grant was supported by Navy contract # N61331-99-C-0040.

References:

1. Statistical Parametric Mapping 99: Wellcome Department of Cognitive Neurology, 2000.
2. **Alsop D.** Correction of ghost artifacts and distortion in echo-planar MR imaging with an iterative reconstruction technique (abstr). *Radiology* 197: 338, 1995.
3. **Alsop DC and Detre JA.** Multisection cerebral blood flow MR imaging with continuous arterial spin labeling. *Radiology* 208: 410-416, 1998.
4. **Alsop DC and Detre JA.** Reduced transit-time sensitivity in noninvasive magnetic resonance imaging of human cerebral blood flow. *J Cereb Blood Flow Metab* 16: 1236-1249, 1996.
5. **Alsop DC and Detre JA.** Reduction of excess noise in fMRI time series data using noise image templates. *Proc Intl Soc for Magn Reson Med* 5: 1687, 1997.
6. **Alsop DC, Detre JA, and Grossman M.** Assessment of cerebral blood flow in Alzheimer's disease by spin- labeled magnetic resonance imaging. *Ann Neurol* 47: 93-100, 2000.
7. **Ashburner J and Friston K.** Multimodal image coregistration and partitioning--a unified framework. *Neuroimage* 6: 209-217, 1997.
8. **Barbier EL, Lamalle L, and Decorps M.** Methodology of brain perfusion imaging. *J Magn Reson Imaging* 13: 496-520, 2001.
9. **Brown MM, Wade JP, and Marshall J.** Fundamental importance of arterial oxygen content in the regulation of cerebral blood flow in man. *Brain* 108 (Pt 1): 81-93, 1985.

10. **Busija DW, Orr JA, Rankin JH, Liang HK, and Wagerle LC.** Cerebral blood flow during normocapnic hyperoxia in the unanesthetized pony. *J Appl Physiol* 48: 10-15, 1980.

11. **Calamante F, Thomas DL, Pell GS, Wiersma J, and Turner R.** Measuring cerebral blood flow using magnetic resonance imaging techniques. *J Cereb Blood Flow Metab* 19: 701-735, 1999.

12. **Chalela JA, Alsop DC, Gonzalez-Atavales JB, Maldjian JA, Kasner SE, and Detre JA.** Magnetic resonance perfusion imaging in acute ischemic stroke using continuous arterial spin labeling. *Stroke* 31: 680-687, 2000.

13. **Clark JM, Sinclair RD, and Lenox JB.** Chemical and nonchemical components of ventilation during hypercapnic exercise in man. *J Appl Physiol* 48: 1065-1076, 1980.

14. **Clark JM, Skolnick BE, Gelfand R, Farber RE, Stierheim M, Stevens WC, Beck G, Jr., and Lambertsen CJ.** Relationship of 133Xe cerebral blood flow to middle cerebral arterial flow velocity in men at rest. *J Cereb Blood Flow Metab* 16: 1255-1262, 1996.

15. **Demchenko IT, Oury TD, Crapo JD, and Piantadosi CA.** Regulation of the brain's vascular responses to oxygen. *Circ Res* 91: 1031-1037, 2002.

16. **Detre JA, Leigh JS, Williams DS, and Koretsky AP.** Perfusion imaging. *Magn Reson Med* 23: 37-45, 1992.

17. **Dietrich HH, Ellsworth ML, Sprague RS, and Dacey RG, Jr.** Red blood cell regulation of microvascular tone through adenosine triphosphate. *Am J Physiol Heart Circ Physiol* 278: H1294-1298, 2000.

18. **Faraci FM and Sobey CG.** Role of potassium channels in regulation of cerebral vascular tone. *J Cereb Blood Flow Metab* 18: 1047-1063, 1998.

19. **Floyd T, Maldjian J, Gonzales-Atavales J, Alsop D, and Detre J.** Test-retest stability with continuous arterial spin labeled(CASL) perfusion MRI in regional measurement of cerebral blood flow. *Ninth Annual Meeting of the ISMRM*, Glasgow, 2001, p. 1569.

20. **Floyd TF, McGarvey M, Ochroch EA, Cheung AT, Augoustides JA, Bavaria JE, Acker MA, Pochettino A, and Detre JA.** Perioperative changes in cerebral blood flow after cardiac surgery: Influence of anemia and aging. *Annals Thorac Surg* In Press, 2003.

21. **Frank LR, Wong EC, Haseler LJ, and Buxton RB.** Dynamic imaging of perfusion in human skeletal muscle during exercise with arterial spin labeling. *Magn Reson Med* 42: 258-267., 1999.

22. **Gessel R.** The regulation of respiration with special reference to the metabolism of the respiratory center and the coordination of the dual function of hemoglobin. *Am J Physiol* 66: 5-49, 1923.

23. **Golanov EV and Reis DJ.** Contribution of oxygen-sensitive neurons of the rostral ventrolateral medulla to hypoxic cerebral vasodilatation in the rat. *J Physiol* 495 (Pt 1): 201-216, 1996.

24. **Iida H, Akutsu T, Endo K, Fukuda H, Inoue T, Ito H, Koga S, Komatani A, Kuwabara Y, Momose T, Nishizawa S, Odano I, Ohkubo M, Sasaki Y, Suzuki H, Tanada S, Toyama H, Yonekura Y, Yoshida T, and Uemura K.** A multicenter validation of regional cerebral blood flow quantitation using

[123I]iodoamphetamine and single photon emission computed tomography. *J Cereb Blood Flow Metab* 16: 781-793, 1996.

25. **Ishikawa T, Kawamura S, Hadeishi H, Suzuki A, Yasui N, and Uemura K.** Cerebral blood flow and oxygen metabolism in hemiparetic patients with chronic subdural hematoma. Quantitative evaluation using positron emission tomography. *Surg Neurol* 43: 130-136; discussion 136-137, 1995.
26. **Kety SS and Schmidt CF.** The determination of cerebral blood flow in man by the use of nitrous oxide in low concentrations. *Am J Physiol* 143: 53-66, 1945.
27. **Kety SS and Schmidt CF.** The effects of altered arterial tensions of carbon dioxide and oxygen on cerebral blood flow and oxygen consumption of normal young men. *J Clin Invest* 27: 484-486, 1948.
28. **Kolbitsch C, Lorenz IH, Hormann C, Hinteregger M, Lockinger A, Moser PL, Kremser C, Schocke M, Felber S, Pfeiffer KP, and Benzer A.** The influence of hyperoxia on regional cerebral blood flow (rCBF), regional cerebral blood volume (rCBV) and cerebral blood flow velocity in the middle cerebral artery (CBFVMCA) in human volunteers. *Magn Reson Imaging* 20: 535-541, 2002.
29. **Lambertsen CJ.** Effects of hyperoxia on organs and their tissues. In: *Extrapulmonary Manifestations of Respiratory Disease*, edited by Robin E. New York: M. Dekker, 1978, p. 239-303.
30. **Lambertsen CJ.** Effects of oxygen at high partial pressure. In: *Handbook of Physiology-Respiration II*, 1965, p. 1027-1046.

31. **Lambertsen CJ.** Invited editorial on "Fast and slow components of cerebral blood flow response to step decreases in end-tidal PCO2 in humans". *J Appl Physiol* 85: 386-387, 1998.

32. **Lambertsen CJ, Ewing JH, Kough RH, Gould R, and Stroud MW.** Oxygen toxicity. Arterial and internal jugular blood gas composition in man during inhalation of air, 100% O2 and 2% CO2 in O2 at 3.5 atmospheres ambient pressure. *J Appl Physiol* 8: 255-263, 1955.

33. **Lambertsen CJ, Kough RH, Cooper DY, Emmel GL, Loeschcke HH, and Schmidt CF.** Comparison of relationship of respiratory minute volume to pCO2 and pH of arterial and internal jugular blood in normal man during hyperventilation produced by low concentrations od CO2 at 1 atmosphere and by O2 at 3.0 atmospheres. *J Appl Physiol* 5: 803-813, 1953.

34. **Lambertsen CJ, Kough RH, Cooper DY, Emmel GL, Loeschcke HH, and Schmidt CF.** Oxygen toxicity: Effects in man of oxygen inhalation at 1 and 3.5 atmospheres upon blood gas transport, cerebral circulation and cerebral metabolism. *J Applied Physiol* 5: 471-485, 1953.

35. **Lassen N and Lane MH.** Validity of internal jugular blood for study of cerebral blood flow and metabolism. *J Applied Physiol* 16: 313-320, 1960.

36. **Lia TQ, Guang Chen Z, Ostergaard L, Hindmarsh T, and Moseley ME.** Quantification of cerebral blood flow by bolus tracking and artery spin tagging methods. *Magn Reson Imaging* 18: 503-512, 2000.

37. **Liu HL, Kochunov P, Hou J, Pu Y, Mahankali S, Feng CM, Yee SH, Wan YL, Fox PT, and Gao JH.** Perfusion-weighted imaging of interictal

hypoperfusion in temporal lobe epilepsy using FAIR-HASTE: comparison with H(2)(15)O PET measurements. *Magn Reson Med* 45: 431-435, 2001.

38. **Loeppky JA, Luft UC, and Fletcher ER.** Quantitative description of whole blood CO2 dissociation curve and Haldane effect. *Respir Physiol* 51: 167-181., 1983.
39. **Mai VM, Bankier AA, Prasad PV, Li W, Storey P, Edelman RR, and Chen Q.** MR ventilation-perfusion imaging of human lung using oxygen-enhanced and arterial spin labeling techniques. *J Magn Reson Imaging* 14: 574-579, 2001.
40. **Ohta H.** [The effect of hyperoxemia on cerebral blood flow in normal humans]. *No To Shinkei* 38: 949-959, 1986.
41. **Pantano P, Baron JC, Lebrun-Grandie P, Duquesnoy N, Bousser MG, and Comar D.** Regional cerebral blood flow and oxygen consumption in human aging. *Stroke* 15: 635-641, 1984.
42. **Pearce WJ.** Mechanisms of hypoxic cerebral vasodilatation. *Pharmacol Ther* 65: 75-91, 1995.
43. **Phillis JW.** Adenosine in the control of the cerebral circulation. *Cerebrovasc Brain Metab Rev* 1: 26-54, 1989.
44. **Pohl U.** Endothelial cells as part of a vascular oxygen-sensing system: hypoxia-induced release of autacoids. *Experientia* 46: 1175-1179, 1990.
45. **Reivich M.** Cerebral circulatory responses to respiratory influences. In: *Cerebral Vascular Diseases*, edited by Toole JF SR, and Whisnant JP. New York: Grune and Stratton, 1968, p. 91-100.

46. **Reivich M.** Regulation of the cerebral circulation. In: *Proceedings of the Congress of Neurological Surgeons*. Baltimore: Williams and Wilkins, 1969, p. 378-418.

47. **Roberts DA, Detre JA, Bolinger L, Insko EK, Lenkinski RE, Pentecost MJ, and Leigh JS, Jr.** Renal perfusion in humans: MR imaging with spin tagging of arterial water. *Radiology* 196: 281-286, 1995.

48. **Roberts DA, Rizi RR, Lipson DA, Ferrante MA, Bearn L, Rolf L, Baumgardner J, Yamomoto A, Hatabu H, Hansen-Flaschen J, Gefter WB, and Schnall MD.** Dynamic observation of pulmonary perfusion using continuous arterial spin-labeling in a pig model. *J Magn Reson Imaging* 14: 175-180, 2001.

49. **Rostrup E, Larsson HB, Toft PB, Garde K, and Henriksen O.** Signal changes in gradient echo images of human brain induced by hypo- and hyperoxia. *NMR Biomed* 8: 41-47, 1995.

50. **Scheinberg P.** The effect of nicotinic acid on the cerebral circulation with observations on extracranial contamination of cerebral venous blood in the nitrous oxide procedure for cerebral blood flow. *Circulation* 1: 1148-1154, 1950.

51. **Sharan M, Gupta S, and Popel AS.** Parametric analysis of the relationship between end-capillary and mean tissue PO2 as predicted by a mathematical model. *J Theor Biol* 195: 439-449, 1998.

52. **Shenkin HA, Harmel MH, and Kety SS.** Dynamic anatomy of the cerebral circulation. *Arch Neurol Psychiat* 60: 240-252, 1948.

53. **Siesjo BK.** Measurements of cerebral oxygen consumption: advantages and limitations. *Eur Neurol* 20: 194-199, 1981.

54. **Silva AC, Kim SG, and Garwood M.** Imaging blood flow in brain tumors using arterial spin labeling. *Magn Reson Med* 44: 169-173, 2000.

55. **Swenson ER, Robertson HT, and Hlastala MP.** Effects of inspired carbon dioxide on ventilation-perfusion matching in normoxia, hypoxia, and hyperoxia. *Am J Respir Crit Care Med* 149: 1563-1569., 1994.

56. **Walsh EG, Minematsu K, Leppo J, and Moore SC.** Radioactive microsphere validation of a volume localized continuous saturation perfusion measurement. *Magn Reson Med* 31: 147-153, 1994.

57. **Wang J, D.C. A, Song HK, Maldjian JA, Tang K, Rabin M, Schnall MD, and Detre JA.** Transit time imaging with flow encoding arterial spin tagging (FEAST). *Magn Reson Med* In Press, 2003.

58. **Waschke KF, Krieter H, Hagen G, Albrecht DM, Van Ackern K, and Kuschinsky W.** Lack of dependence of cerebral blood flow on blood viscosity after blood exchange with a Newtonian O2 carrier. *J Cereb Blood Flow Metab* 14: 871-876, 1994.

59. **Watson NA, Beards SC, Altaf N, Kassner A, and Jackson A.** The effect of hyperoxia on cerebral blood flow: a study in healthy volunteers using magnetic resonance phase-contrast angiography. *Eur J Anaesthesiol* 17: 152-159, 2000.

60. **Wolf RL, Alsop DC, Levy-Reis I, Meyer PT, Maldjian JA, Gonzalez-Atavales J, French JA, Alavi A, and Detre JA.** Detection of mesial temporal lobe hypoperfusion in patients with temporal lobe epilepsy by use of arterial spin labeled perfusion MR imaging. *AJNR Am J Neuroradiol* 22: 1334-1341, 2001.

61. **Wong EC.** Potential and Pitfalls of Arterial Spin Labeling Based Perfusion Imaging Techniques for MRI. In: *Functional MRI*, edited by Moonen CTW and Bandettini PA. Heidelberg: Springer-Verllag, 1999, p. 63-69.

62. **Wong EC, Buxton RB, and Frank LR.** Implementation of quantitative perfusion imaging techniques for functional brain mapping using pulsed arterial spin labeling. *NMR Biomed* 10: 237-249, 1997.

63. **Wong EC, Buxton RB, and Frank LR.** Quantitative perfusion imaging using arterial spin labeling. *Neuroimaging Clin N Am* 9: 333-342, 1999.

64. **Xu Y, Liachenko S, and Tang P.** Dependence of early cerebral reperfusion and long-term outcome on resuscitation efficiency after cardiac arrest in rats. *Stroke* 33: 837-843, 2002.

65. **Ye FQ, Berman KF, Ellmore T, Esposito G, van Horn JD, Yang Y, Duyn J, Smith AM, Frank JA, Weinberger DR, and McLaughlin AC.** H(2)(15)O PET validation of steady-state arterial spin tagging cerebral blood flow measurements in humans. *Magn Reson Med* 44: 450-456, 2000.

Figure Legends:

Fig. 1 - Colorized CASL-Perfusion MRI images with scale depicting CBF changes in response to Air, Air - 4%CO_2, Air - 6%CO_2, 100% O_2, 96% O_2 - 4%CO_2, and 94% O_2 - 6%CO_2.

Fig. 2 - Cerebral blood flow is plotted versus arterial pCO_2 for the Air and Hyperoxia runs. Means and standard error bars are presented for CBF and pCO_2 values for each gas. Means are connected describing curves representing the CBF response to pCO_2 in the presence of air and hyperoxia.

Fig. 3 - Absolute ($\Delta CBF_{4\%-6\%}$) and relative (% $\Delta CBF_{4\%-6\%}$) changes in CBF from baseline measurements made on 4% and 6% CO_2 in air background to measurements made on 4% and 6% CO_2 in oxygen background are plotted versus baseline CBF measurements made on 4-6% CO_2 in air background.

Fig. 4(a-c) - Actual (measured) CBF versus Predicted (model derived) CBF for global (a), gray matter (b) and white matter (c) along with 95% confidence intervals (- - - -).

Table Legends:

Table 1

Values are presented as Mean ± (SD).

[1]Significance in comparison between Air (21% O_2) and 100% O_2.

[2]Significance in comparison between Air - 4%CO_2 and 96%O2 - 4%CO_2.

[3]Significance in comparison between Air - 6%CO_2 and 94%O2 - 6%CO_2.

Table 2

N=14, includes measurements of the change in CBF (ΔCBF) from seven (7) subjects when breathing Air - 4%CO_2 vs. 96%O_2 - 4%CO_2 and Air - 6%CO_2 versus 94%O_2 - 6%CO_2.

Table-1. Arterial pCO_2, pO_2, O_2 Content, and CBF by Inspired Gas.

Inspired Gas	pCO_2 (mmHg)	pO_2 (mmHg)	CaO_2 (ml/dl)	CBF_{Global} (ml/100g/min)	CBF_{Gray} (ml/100g/min)	CBF_{White} (ml/100g/min)
Air(21%O_2) [1]	43.3(1.8) (p=.01)	91.7(6.8) (p<.0001)	17.9(.8) (p<.0001)	53.6(6.8) (p<.0001)	68.6(8.9) (p<.0001)	39.6(7.7) (p=.003)
Air-4%CO_2 [2]	46.4(1.7) (p=.25)	127.0(5.4) (p<.0001)	18.5(.9) (p=.0002)	56.1(10.5) (p=.0008)	73.5(13.7) (p=.003)	39.8(11.8) (p=.03)
Air-6%CO_2 [3]	52.1(1.6) (p=.13)	144.5(6.6) (p<.0001)	18.7(.8) (p<.0001)	70.1(6.4) (p<.0001)	90.4(11.9) (p<0001)	47.6(4.5) (p=.006)
100%O_2	40.2(3.3)	576.7(18.9)	20.3(1.1)	36.1(4.9)	46.6(5.3)	27.8(3.8)
96%O_2-4%CO_2	45.6(2.2)	580.2(19.6)	20.2(.8)	40.0(3.1)	50.3(5.8)	30.5(5.1)
94%O_2-6%CO_2	51.1(2.0)	579.4(10.6)	20.3(.8)	49.6(5.4)	62.4(8.3)	35.2(8.6)

Table 2. ΔCBF Multiple Regression Analysis-Terms and Coefficients

Term	*Coefficient*	*P=*	*Power(β) (α=.05)*	*Least Significant Number (α=.05)*
Intercept	-14	.0029	.85	**8**
$CBF_{AIR-4\%-6\%}$	.70	<.0001	>.99	6
ΔpO_2	-.25	.008	.71	9
ΔpCO_2	1.0	.17	.12	28

Figure- 1

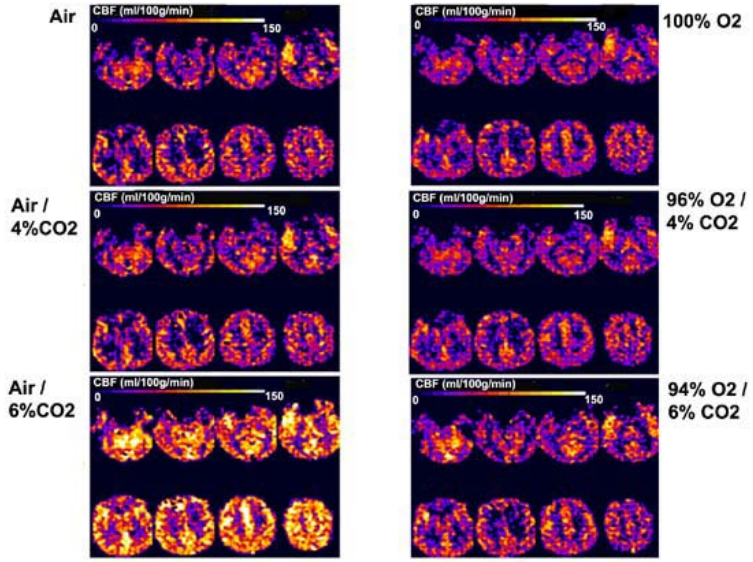

Figure-2

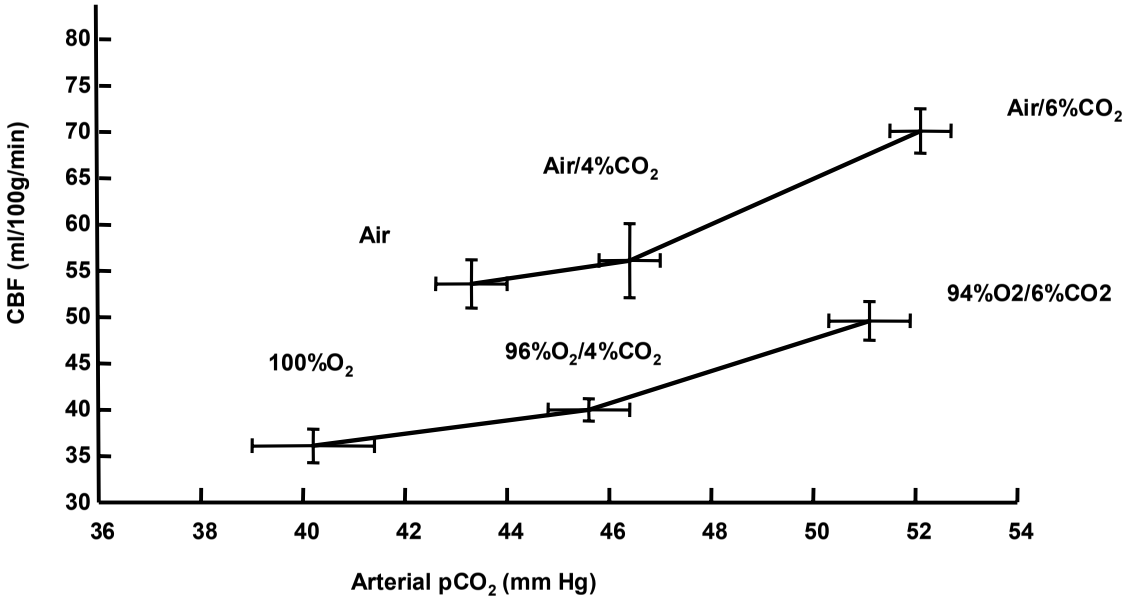

Figure-3

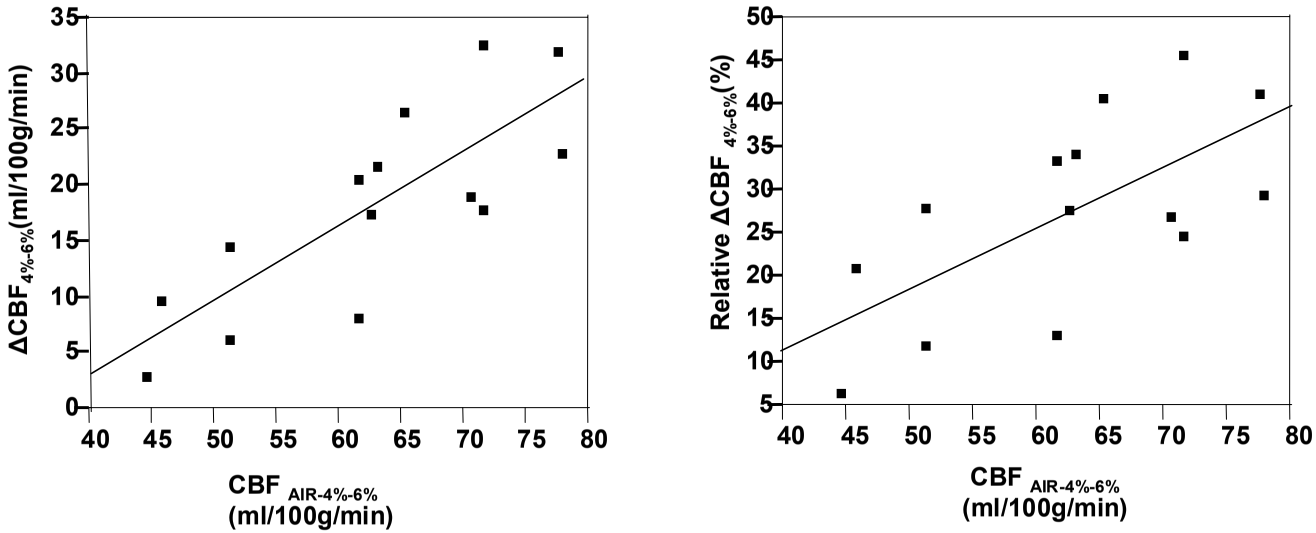

Figure-4